Hauser-Feshbach Analysis of Fast Neutron-Induced Reactions on Chlorine

Kenneth Hanselman[1,*], *Sean* Kuvin[1], *Hye Young* Lee[1], *Toshihiko* Kawano[1], *Scott* Essenmacher[1], *Panagiotis* Gastis[1], *Heshani* Jayatissa[1], *Tommy* Cisneros[2], *Matthew* Wargon[2], and *Lukas* Zavorka[3]

[1]Los Alamos National Laboratory, Los Alamos, NM 87545, USA
[2]TerraPower LLC, Bellevue, WA 98008, USA
[3]Oak Ridge National Laboratory, Oak Ridge, TN 37830, USA

Abstract. Neutron-induced reactions on ^{35}Cl have recently been measured and analyzed in a Hauser-Feshbach framework at Los Alamos National Laboratory. Particular focus has been applied to the "fast" energy range above 100 keV, where these reactions become important for applications like CLYC (Cs_2LiYCl_6:Ce) detector characterization and the development of molten chloride fast reactors. However, challenges to applying a purely statistical analysis to this mass range have presented themselves in the form of cross section fluctuations and deviations due to low-mass structure. In this paper, these challenges and their current solutions will be highlighted, as well as preliminary extensions of the analysis to neighboring isotopes and future plans to extend the measurements down to thermal energies.

1 Introduction

Recently, authors from Los Alamos National Laboratory (LANL) and TerraPower LLC (TP) have presented new experimental data for ^{35}Cl(n,p) and ^{35}Cl(n,α) fast-energy cross sections, as well as a Hauser-Feshbach reanalysis of all relevant n + ^{35}Cl channels using these new data [1]. This analysis has formed the basis for a full nuclear data evaluation of chlorine isotopes at fast-neutron energies as part of a Gateway for Innovation in Nuclear (GAIN) collaboration between LANL and TP. The new evaluation, labeled hereafter as "LANL-TP", benefits the growing number of applications which rely on chlorine nuclear data, for example TP's Molten Chloride Reactor Experiment (MCRE) [2]; modern neutron detectors (*e.g.* Cs_2LiYCl_6:Ce, or "CLYC") used in basic science and applied diagnostics [3, 4]; and reaction networks for nuclear astrophysics [5, 6].

Presented in this work are some of the first extensions of the analysis of Ref. [1] to neighboring isotopes of ^{35}Cl, specifically ^{37}Cl and ^{39}K. These are the first steps toward a fuller cross-isotope evaluation in this challenging mass range. Section 2 summarizes these results while Section 3 discusses them in the framework of the physical models. Section 4 presents a summary, as well as a look ahead to future measurements at LANL to extend the re-evaluation down to thermal incident energies.

2 Results

The final fast-energy analysis of Ref. [1] was a combination of adjustments to default optical model potentials (OMPs), nuclear level densities, and preequilibrium state densities as defined in the Hauser-Feshbach code CoH_3 [7]. That work was tuned solely to channels of ^{35}Cl. To judge its consistency and applicability across the mass range, all relevant adjustments (principally OMPs and preequilibrium) were carried over to analogous calculations for ^{37}Cl and ^{39}K, for which there are some available data. These are shown in Figure 1 for the (n,total) and (n,p) reactions specifically, compared to default calculations using the unadjusted global OMP sets of Koning and Delaroche [8] and Kunieda *et al.* [9].

3 Discussion

In general, the LANL-TP analysis for (n,p) translates well across isotopes, representing improvement over the base models. Two improvements in particular stand out: the reduction in cross section in the ~few MeV region through reduced OMP absorption, and the increase in cross section at much higher energies due to preequilibrium contributions.

The necessary increase in preequilibrium strength through the nucleon state densities was a finding of Ref. [1], and was rationalized to account for higher-energy reaction models not included in the analysis, *e.g.* direct charge-exchange. The fact that the ^{37}Cl(n,p) data also favor this adjustment is further support for this argument, as such an effect would translate across the mass range.

Meanwhile, the reduction in absorption is clearer in the ^{39}K(n,p) cross section. To explain this, it is helpful to examine the qualitative structural behavior of these isotopes. Figure 2 shows combinatorial level densities of the relevant compound nuclear systems calculated with the Finite Range Droplet Model (FRDM) [10]. Of note is that all three densities lie below the statistical predictions of the

*e-mail: khanselman@lanl.gov

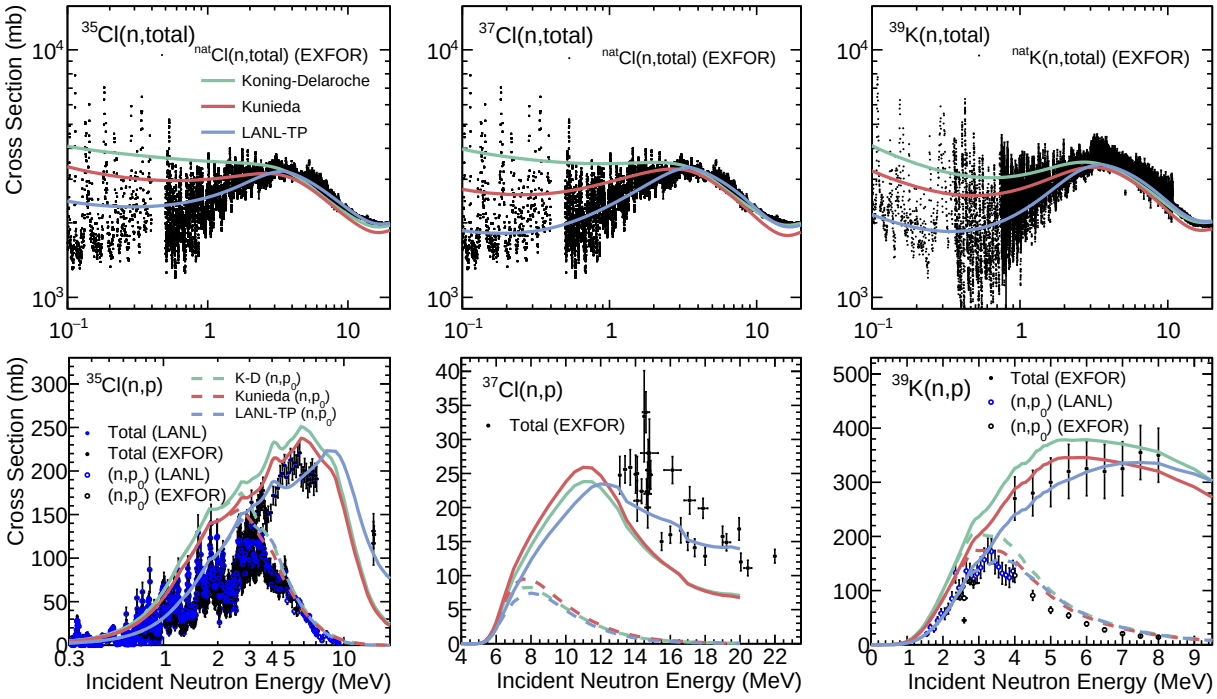

Figure 1. Summary of the impact of the new LANL-TP analysis (solid blue, Ref. [1]) on various isotopes in chlorine's mass range. In comparison are shown default calculations using unmodified global OMP sets for the neutron and proton: Koning & Delaroche (solid green, Ref. [8]) and Kunieda *et al.* (solid red, Ref. [9]). Select data pulled from EXFOR are in black while those measured in recent years at LANL [1, 11] are in blue. The LANL data for ^{39}K(n,p) are preliminary and will be part of an upcoming publication.

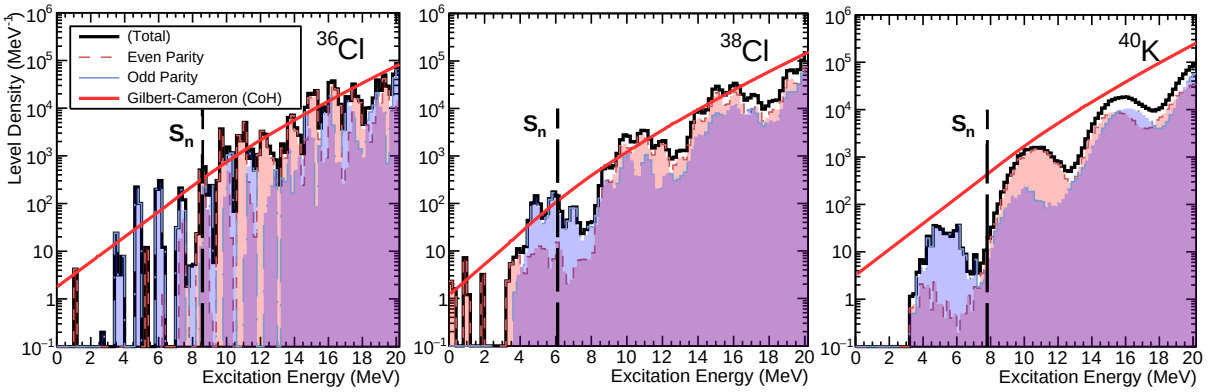

Figure 2. FRDM combinatorial calculations for the level densities of relevant compound systems. Contrasted against the total (black) are the individual components for even (dashed red) and odd (dashed blue) parities. Configurations up to 5p-5h are included. Also noted are the neutron separation energies S_n and the Gilbert-Cameron (H-F) level densities calculated by CoH (dashed-black verticals and solid red curves respectively).

Gilbert-Cameron model, due to proximity to the N=Z=20 shell gap. Thus all three nuclei require less neutron absorption than that suggested by global, systematic studies, which are often the defaults in nuclear reaction codes.

Also of note are the differences in structure of the level densities themselves. ^{36}Cl presents a level density more prone to short-scale fluctuations, visible in the ^{35}Cl(n,p) cross section of Figure 1 as many sharp dips and peaks as high as 3–5 MeV in incident energy. One candidate for this are the irregular spacings of the single-particle occupancies as nucleons are removed from the system, an effect also seen in the FRDM calculations. Practically, these features were treated in Ref. [1] through a direct fitting procedure, to capture the most macroscopic deviations which might impact applications. For ^{39}K this does not seem to be as necessary, though more experimental data are required to determine if this also holds true for ^{37}Cl.

4 Summary & Future Work

It has been shown that the analysis of Ref. [1] can be extended beyond ^{35}Cl to neighboring isotopes. In particular, both the reduction in neutron absorption and the increase

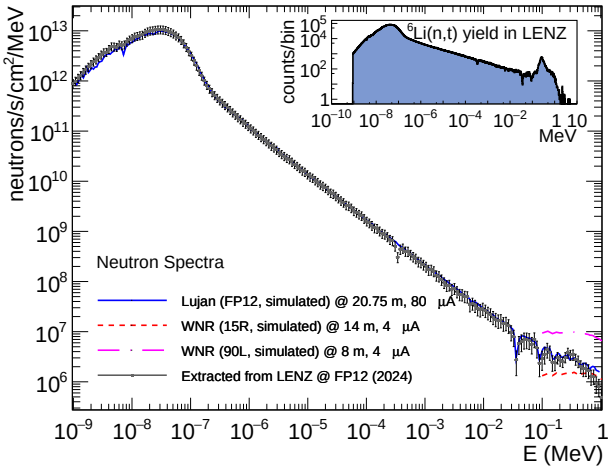

Figure 3. Comparison of simulated and extracted neutron beam fluence at FP12 at the Lujan Scattering Center. The black data points were extracted from LENZ data taken in February 2024 using the inset measured ^{6}Li(n,t) cross section yield as reference. In addition to an analogous MCNP simulation in solid blue, similar calculations for the 15R and 90L flight paths at WNR (used in Ref. [1]) are shown as the dashed curves, highlighting the potential overlap between measurements.

in preequilibrium strength appear to translate within the mass region.

However, a true multi-isotopic study will require more data. For example, ^{37}Cl(n,p) and (n,α), having widely discrepant data above 13 MeV and none below, would be measurable with the Low-Energy (n,Z) (LENZ) instrument at the WNR flight paths, as mentioned in Ref. [1]. Additionally, in support of the priorities of the Nuclear Criticality Safety Program [12], there is an ongoing effort at LANL to measure new ^{35}Cl(n,p) data down to thermal energies, using LENZ with the moderated neutron source at the Lujan Scattering Center. Examples of the neutron fluence at the anticipated flight path (FP12) are shown in Figure 3. Included are both simulated results using MCNP6 and preliminary data extracted from LENZ during the 2023 LANSCE run cycle. The relative incident neutron spectrum was extracted using the measured yield of the ^{6}Li(n,t) reaction in a 65 μm Micron S1 double-sided silicon detector covering lab angles 117.4°–136.1°. The target was an enriched 200 μg/cm^2 ^{6}LiF foil. This yield was folded with the appropriate differential cross section data from the latest ENDF/B-VIII.1 library, then normalized to the simulated result to compare the energy-dependent shape of the incident neutron flux. This was an important first step toward new measurements at FP12, as it is the first characterization of the flight path after the replacement of the spallation neutron source with the Mark-IV design [13].

Further analysis on this preliminary data is ongoing, with the goal of informing upcoming Lujan experiments. By combining results from Lujan and WNR, LENZ will be able to provide data for ^{35}Cl(n,p) across multiple orders of magnitude in incident energy, granting even greater confidence in future evaluation of this and related isotopes.

Acknowledgement

This work was supported by the Nuclear Criticality Safety Program, funded and managed by the National Nuclear Security Administration for the Department of Energy. Funding was also provided in part by the DOE's Advanced Simulation and Computing Program. This work was carried out under the auspices of the National Nuclear Security Administration of the US Department of Energy at Los Alamos National Laboratory under Contract No. 89233218CNA000001. The authors would like to thank Josef Svoboda of LANL for providing the MCNP neutron spectra.

References

[1] K. Hanselman *et al.*, Phys. Rev. C **110**, 024609 (2024). 10.1103/PhysRevC.110.024609

[2] G. Palmiotti *et al.* OSTI No. 1891907, Report No. INL/CON-21-64838-Rev000, Idaho National Lab. (INL), Idaho Falls, ID, United States (2021). https://www.osti.gov/biblio/1891907

[3] T. Brown *et al.*, Nucl. Instrum. Meth. Phys. Res. A **954**, 161123 (2020). 10.1016/j.nima.2018.08.082

[4] L. Soundara-Pandian *et al.*, IEEE Trans-act. on Nuc. Sci. **64**, 1744–1748 (2017). 10.1109/TNS.2017.2691552

[5] P. E. Koehler, Phys. Rev. C **44**, 1675 (1991). 10.1103/PhysRevC.44.1675

[6] S. Druyts *et al.* Nucl. Phys. A **573**, 291 (1994). 10.1016/0375-9474(94)90172-4

[7] T. Kawano *et al.* J. Nuc. Sci. & Tech. **43**, 1–8 (2006). 10.1080/18811248.2006.9711062

[8] A. J. Koning and J. P. Delaroche, Nuc. Phys. A **713**, 231–310 (2003). 10.1016/S0375-9474(02)01321-0

[9] S. Kunieda *et al.*, J. Nucl. Sci. & Tech. **44**, 838–852 (2007). 10.1080/18811248.2007.9711321

[10] P. Möller *et al.*, At. Data Nucl. Data Tables **109-110**, 1 (2016). 10.1016/j.adt.2015.10.002

[11] S. A. Kuvin *et al.*, Phys. Rev. C **102**, 024623 (2020). 10.1103/PhysRevC.102.024623

[12] "Five Year Execution Plan for the Mission and Vision of the United States Department of Energy Nuclear Criticality Safety Program," Appendix B, 2022. https://ncsp.llnl.gov/program-management/ncsp-five-year-execution-plan [Accessed: 14-Oct-2024].

[13] L. Zavorka *et al.* Nucl. Instrum. Meth. Phys. Res. A **1040**, 167210 (2022). 10.1016/j.nima.2022.167210